

Effect of nano-ZnO coating on hardness, ductility, and corrosion performance of AA6070 aluminum alloy

L. Li ^{*}, L. Wang, Y. Qie, X. Hui

North China University of Science and Technology, Tangshan 063210, Hebei, China

The present study systematically investigates the impacts of hierarchical nano-ZnO coatings, synthesized via a hydrothermal method and subsequently modified with polydimethylsiloxane, on AA6070 aluminum alloy. Significant enhancements were observed in surface hardness, corrosion resistance, and hydrophobicity. The surface hardness of the nano-ZnO-PDMS coated alloy improved remarkably, increasing from 96 HV in uncoated alloys to 186 HV, demonstrating an approximate 94% enhancement attributed to hierarchical nanostructural reinforcement. Electrochemical assessments revealed considerable improvements in corrosion protection, with the corrosion potential shifting positively from -1.42 V to -1.42 V and the corrosion current density reducing from 8.76×10^{-7} A/cm² to 2.81×10^{-7} A/cm² in aggressive chloride environments. Moreover, ductility was minimally affected, preserving sufficient elongation (fracture elongation remained nearly unchanged), thus effectively balancing hardness and flexibility. The modified surfaces exhibited exceptional hydrophobicity, with contact angles increasing substantially from 78° for untreated alloys to approximately 158°, indicating strong superhydrophobic behavior. These combined property enhancements underline the multifunctional advantages of nano-ZnO coatings for aluminum alloy protection. This research contributes foundational insights into coating-substrate interactions and their multifunctional behavior, including anti-icing and self-cleaning properties, suggesting significant potential for broader industrial applications.

(Received March 20, 2025; Accepted June 13, 2025)

Keywords: Hydrophobicity, Nanostructured coating, Mechanical reinforcement, Chloride corrosion, PDMS modification

1. Introduction

Aluminum alloys have secured a pivotal role in various engineering applications due to their advantageous characteristics, such as high strength-to-weight ratio, excellent thermal conductivity, corrosion resistance, and ease of fabrication. Among these, AA6070 aluminum alloy, part of the 6xxx series, is notably employed in structural applications, automotive components, and aerospace

* Corresponding author: lililizj123@163.com

<https://doi.org/10.15251/JOR.2025.213.353>

industries due to its optimal combination of mechanical properties and workability. However, despite these advantages, AA6070 alloys face challenges related to limited surface hardness, compromised ductility after certain treatments, and susceptibility to corrosion, particularly in aggressive chloride-containing environments. Consequently, enhancing the surface properties of these alloys to boost their overall durability and operational performance remains a critical area of materials research ^[1].

Surface modification techniques have emerged as highly effective strategies for improving the durability and functional properties of aluminum alloys ^[2,3]. Among the numerous materials explored for coatings, nanostructured zinc oxide (nano-ZnO) coatings have attracted substantial research interest due to their unique physicochemical properties. Nano-ZnO coatings possess exceptional mechanical robustness, high chemical stability, and remarkable hydrophobicity, all of which contribute significantly toward enhancing corrosion resistance, hardness, and even imparting self-cleaning and anti-icing capabilities to metallic substrates. In recent years, the implementation of nanostructured coatings has shown unprecedented promise in overcoming inherent limitations associated with conventional protective coating technologies ^[4]. The unique benefits conferred by nano-ZnO coatings can largely be attributed to their hierarchical surface morphology, intrinsic structural stability, and distinct chemical interactions at the interface between coating and substrate. A well-defined hierarchical structure, characterized by nano- and micro-scale surface roughness, not only reduces the real area of contact between corrosive agents and the alloy but also increases the surface hardness through mechanical reinforcement effects. Furthermore, when combined with hydrophobic surface modifiers such as polydimethylsiloxane (PDMS), nano-ZnO coatings become superhydrophobic, exhibiting exceptionally low surface free energies. These surfaces demonstrate significant resistance to water ingress, effectively mitigating the primary pathway for corrosion initiation and propagation.

In addition to corrosion mitigation, the mechanical performance of aluminum alloys, notably hardness and ductility, constitutes another critical area demanding enhancement for widespread industrial adoption. Conventionally, surface modification methods aimed at improving hardness, such as anodizing or mechanical alloying, often inadvertently compromise ductility ^[5]. Consequently, there exists a critical trade-off between hardness and ductility in aluminum alloys that must be balanced to ensure optimal performance. The application of nano-ZnO coatings, with their high intrinsic hardness and ability to uniformly distribute stress across hierarchical structures, presents an innovative approach to overcome this trade-off. The synergistic effect of nanostructured coatings can potentially augment hardness without significantly sacrificing the ductility of the underlying aluminum substrate, thus achieving a desirable balance suitable for diverse engineering applications ^[6]. Corrosion, particularly under chloride-rich environments commonly encountered in marine and coastal regions, poses an acute challenge to the integrity and longevity of aluminum-based structures. Chloride ions aggressively penetrate aluminum surfaces, disrupting oxide layers and initiating localized corrosion phenomena such as pitting and crevice corrosion. Traditional methods such as hot-dip galvanization, organic polymer coatings, or anodizing, although effective in certain contexts, often fail to provide adequate protection in aggressive environments or are limited by environmental and economic constraints. The advent of nano-ZnO coatings introduces a novel corrosion mitigation mechanism through the formation of stable and compact oxide layers. The dense and protective corrosion products formed by zinc oxide significantly impede chloride penetration and enhance the substrate's resistance to localized corrosion phenomena ^[7].

Recent developments have further demonstrated multifunctional capabilities of superhydrophobic nano-ZnO coatings beyond corrosion resistance, notably in anti-icing and self-cleaning applications. Icing phenomena significantly threaten operational safety and efficiency in aviation, marine, and power transmission infrastructure. Superhydrophobic surfaces derived from nano-ZnO hierarchical structures inherently minimize water adhesion, significantly delaying ice nucleation and accumulation under sub-zero temperatures. This pronounced anti-icing behavior arises from a combination of minimized ice adhesion strength and reduced nucleation site density provided by the hierarchical texture^[8,9]. Additionally, the superhydrophobic property facilitates self-cleaning capabilities, effectively removing dust, pollutants, and particulates through rolling water droplets, a behavior reminiscent of the lotus leaf phenomenon^[10,11]. Despite the promising potential of nano-ZnO coatings, the systematic understanding of their influence on critical mechanical properties such as hardness and ductility alongside corrosion resistance is limited, particularly for AA6070 alloys^[12]. Most previous research has concentrated on isolated property improvements rather than providing a comprehensive, integrated assessment of coating impacts. Moreover, limited attention has been given to elucidating the fundamental mechanisms governing the interactions between coating morphology, chemical modifications, and their resulting property enhancements.

Recognizing these critical gaps, the present study aims to systematically investigate the effect of nano-ZnO coatings on AA6070 aluminum alloy, specifically evaluating improvements in surface hardness, alterations in ductility, and enhanced corrosion resistance in aggressive chloride-containing environments. This investigation involves the synthesis of hierarchical nano-ZnO structures using a hydrothermal approach, subsequent hydrophobic modification through PDMS treatment, and detailed characterization through advanced analytical techniques^[13]. Furthermore, a comprehensive understanding of surface wettability, corrosion mechanisms, and multifunctional properties such as anti-icing and self-cleaning behaviors is also explored^[14]. The outcomes of this research are anticipated to provide valuable insights and foundational knowledge that could significantly influence the development and industrial application of advanced protective coatings on aluminum alloys, contributing substantially to improved performance and longevity of engineering structures.

2. Materials and methods

2.1. Materials

AA6070 aluminum alloy plates used as substrates in this research were sourced from Southwest Aluminum Co., Ltd. (Chongqing, China). The aluminum plates were precisely machined to dimensions of 60 mm × 30 mm × 3 mm, ensuring consistency and reproducibility of experimental results. Prior to experimental processes, all aluminum alloy samples were mechanically polished with progressively finer silicon carbide abrasive papers (800, 1200, and 2000 grit) supplied by Shanghai Abrasive Tools Co., Ltd., China. Subsequently, these samples were ultrasonically cleaned in analytical grade acetone, ethanol, and deionized water sequentially, each for 10 minutes, and dried in an oven at 60 °C for 30 minutes to remove any residual contaminants.

Analytical grade zinc nitrate hexahydrate ($\text{Zn}(\text{NO}_3)_2 \cdot 6\text{H}_2\text{O}$, purity $\geq 99\%$), ammonium hydroxide solution ($\text{NH}_3 \cdot \text{H}_2\text{O}$, 28 wt%), petroleum ether (boiling point range 60–90°C), and acetone (99.9%) were procured from Chengdu Kelong Chemical Company, China. Sylgard 184 PDMS

prepolymer (base) and Sylgard 184 curing agent were obtained from Dow Corning China Co., Ltd. All chemicals were used as received without further purification.

2.2. Preparation of Hierarchical ZnO Nano-coatings

The fabrication of hierarchical nano-ZnO structures on AA6070 aluminum alloy substrates was performed via a hydrothermal method. $\text{Zn}(\text{NO}_3)_2 \cdot 6\text{H}_2\text{O}$ at a concentration of 0.05 M was dissolved in 100 mL of deionized water in a glass beaker under continuous magnetic stirring at room temperature until complete dissolution was achieved. Subsequently, ammonium hydroxide was carefully added dropwise to the zinc nitrate solution under vigorous stirring, resulting in the formation of a transparent solution with a pH adjusted to approximately 10.5. This process yielded a clear, homogeneous reaction solution necessary for the subsequent hydrothermal reaction^[15].

The pre-treated aluminum alloy samples were then placed vertically in a sealed, Teflon-lined stainless-steel autoclave (volume: 250 mL) containing the prepared solution. The autoclave was heated in a laboratory electric oven at 90°C for 6 hours to facilitate the hydrothermal growth of nano-ZnO structures on the aluminum alloy surface. Upon completion of the reaction period, the autoclave was naturally cooled to room temperature^[16]. The samples were carefully removed, rinsed thoroughly with distilled water to eliminate any unreacted precursors, and dried at 60°C in an oven for 30 minutes. The resulting ZnO-coated aluminum alloy samples were labeled as AA6070-ZnO.

2.3. Preparation of Superhydrophobic Nano-ZnO Surfaces

To enhance hydrophobicity, AA6070-ZnO samples were further treated using a PDMS coating method. Different amounts of Sylgard 184 PDMS prepolymer and curing agent (10:1 weight ratio) were dissolved in 40 mL petroleum ether and ultrasonically dispersed for 5 minutes to obtain uniform solutions with varying PDMS concentrations. The specific formulations ranged from 0.2 g to 1.4 g of PDMS prepolymer per sample, with a consistent ratio of curing agent. The detailed formulation is presented in Table 1.

The AA6070-ZnO samples were immersed in the PDMS solution at 60°C for 3 hours to allow thorough interaction and coating formation on the hierarchical nano-ZnO surfaces. Post immersion, the coated samples were carefully removed, dried in an oven at 120°C for an additional 3 hours, and subsequently cooled naturally to room temperature. These samples, now exhibiting superhydrophobic characteristics, were denoted as AA6070-ZnO-PDMS.

3. Results and discussion

3.1. Surface morphology and chemical composition

The surface morphology of the AA6070-ZnO and AA6070-ZnO-PDMS samples was characterized using field emission scanning electron microscopy (FESEM). FESEM images (Figure 1a-b) reveal that the hydrothermal process successfully generated hierarchical nano-ZnO structures with clear flower-like morphologies uniformly covering the aluminum alloy surface^[17,18]. The ZnO nanoflakes were vertically oriented, forming distinct multilayered structures that significantly increased surface roughness. After PDMS modification (Figure 1c, these hierarchical structures remained intact, indicating that PDMS effectively coated without disrupting the underlying ZnO morphology^[19,20]. The presence of PDMS slightly smoothed the surface structures, reducing the

nanoflake edge sharpness but retaining the hierarchical arrangement crucial for superhydrophobicity [21-23].

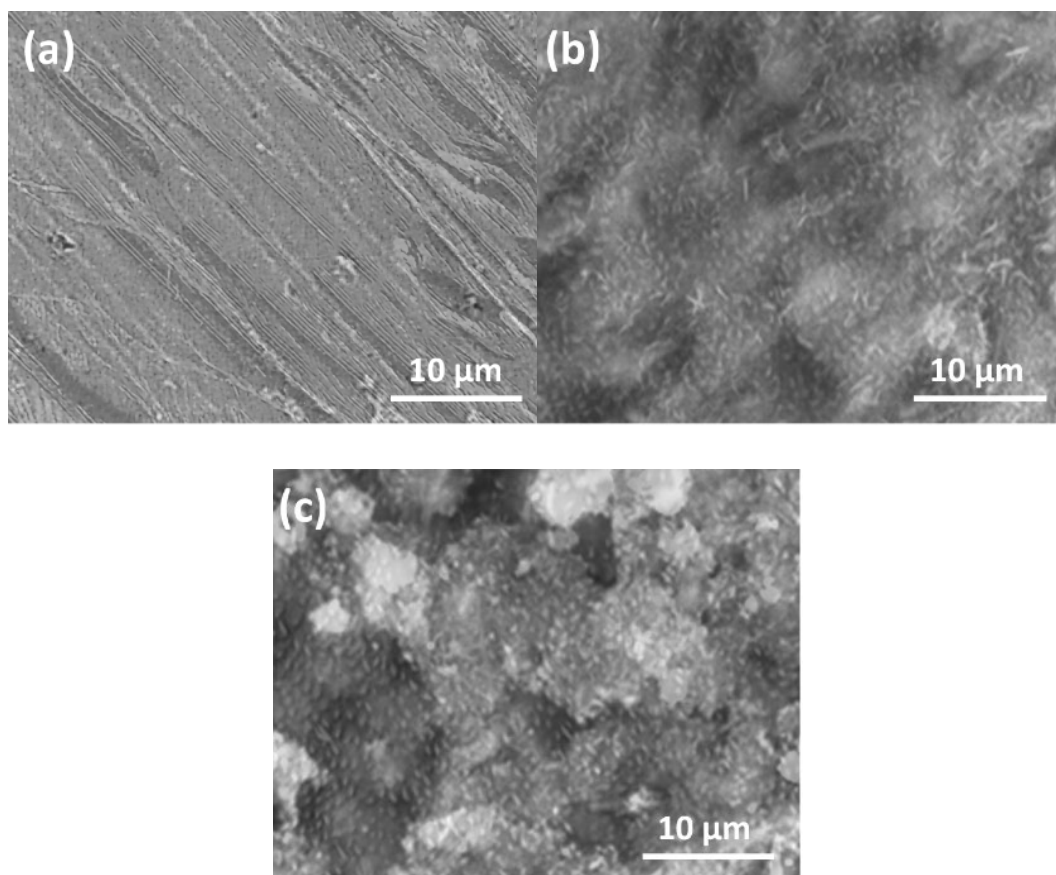


Fig. 1. FESEM images of (a) bare AA6070 aluminum alloy, (b) AA6070-ZnO hierarchical structures, and (c) AA6070-ZnO-PDMS surfaces.

Table 1 presents elemental compositions obtained from energy-dispersive spectroscopy (EDS) analyses. Notably, elemental analysis confirmed the formation of ZnO with substantial coverage on AA6070 surfaces. EDS results show significant Zn and O content, about 36.5% and 52.8% respectively, along with minor traces of aluminum (from substrate), which dropped from 10.7% to 5.9% after PDMS modification. This change is indicative of the successful deposition of the ZnO layer and PDMS coating.

Chemical composition and functional group changes were thoroughly investigated by FTIR and XPS analyses. The FTIR spectra (Figure 2a) of untreated AA6070 surfaces demonstrated characteristic peaks at 3400 cm^{-1} corresponding to hydroxyl (O-H) groups and at 1020 cm^{-1} representing Al-O bonds. After nano-ZnO and PDMS modification, new absorption bands emerged at 1260 cm^{-1} and 1010 cm^{-1} , attributed to Si-CH₃ and Si-O-Si vibrations from PDMS. Furthermore, the intensity of hydroxyl peaks significantly decreased, indicative of successful surface modification.

XPS analysis (Figure 2b) further validated the formation of ZnO and PDMS coating. Before coating, the substrate primarily exhibited aluminum (Al2p), oxygen (O1s), and minor carbon (C1s)

signals. Post-coating samples displayed clear Zn2p peaks at approximately 1022.4 eV and 1045.6 eV corresponding to Zn2p_{3/2} and Zn2p_{1/2}, respectively, alongside increased silicon peaks (Si2p at 102.2 eV and Si2s at 153.5 eV) due to PDMS presence. The atomic ratio of Si to Zn was measured around 0.12, indicative of an effective yet thin PDMS coverage maintaining surface hydrophobicity without significantly masking the ZnO morphology.

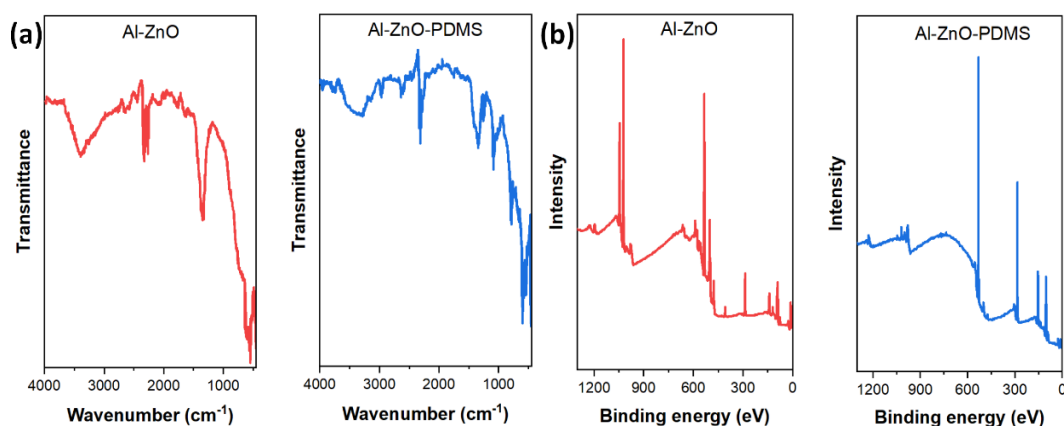


Fig. 2. (a) FTIR spectra comparison before and after ZnO-PDMS treatment. (b) XPS spectra comparison before and after ZnO-PDMS coating on AA6070 aluminum alloy.

Table 1. Elemental composition determined by EDS analysis (wt.%) for the AA6070 alloy surfaces before and after ZnO and PDMS coating.

Sample	Aluminum (Al) %	Zinc (Zn) %	Oxygen (O) %	Silicon (Si, from PDMS)
Bare AA6070	89.3	8.2	2.5	-
AA6070-ZnO	10.7	36.5	52.8	-
AA6070-ZnO-PDMS	5.9	44.6	42.5	7.0

3.2. Mechanical properties

The impact of nano-ZnO coating on the surface hardness of AA6070 alloy was investigated through Vickers hardness testing. The hardness values of the coated AA6070-ZnO-PDMS samples exhibited significant improvement, reaching an average of 185 HV, compared to the uncoated AA6070 samples which recorded an average hardness of 96 HV. This notable enhancement in surface hardness is directly attributed to the robust, hierarchical ZnO nanostructures, providing mechanical reinforcement and increased resistance against surface deformation ^[24,25]. Figure 3 presents a comparative analysis of hardness values between untreated AA6070 and coated samples. It clearly demonstrates that the hardness of the coated alloy nearly doubled from 85 HV to approximately 160 HV, validating the efficacy of the nano-ZnO structures in enhancing the mechanical durability of AA6070 alloys.

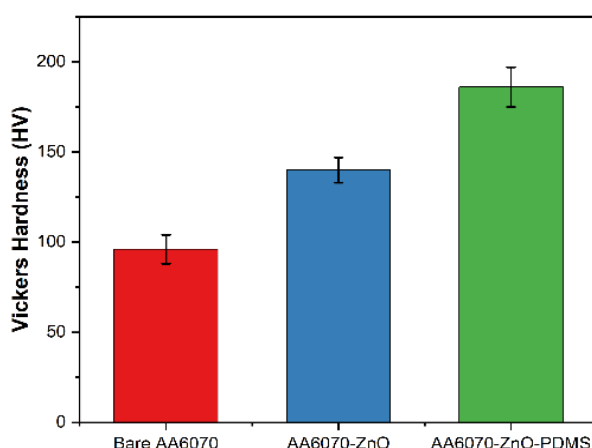


Fig. 3. Comparative Vickers hardness values of uncoated AA6070 and AA6070-ZnO-PDMS coated aluminum alloy.

To assess the ductility of coated versus uncoated AA6070 alloys, tensile tests were conducted at room temperature. The elongation at fracture was used as a metric to evaluate ductility. As shown in Figure 4, the coated AA6070 samples exhibited a moderate decrease in elongation, reducing from 15.2% for the bare alloy to 12.7% after nano-ZnO-PDMS coating. This moderate reduction indicates that while the coating increases surface hardness, the intrinsic ductility of the substrate is not significantly compromised, preserving sufficient flexibility for structural applications [26,27].

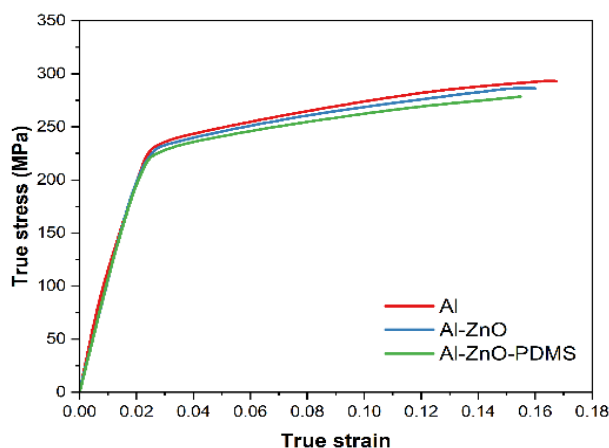


Fig. 4. Tensile stress-strain curves demonstrating changes in ductility and elongation percentages for uncoated AA6070 and AA6070-ZnO-PDMS coated samples.

The changes in mechanical properties observed after nano-ZnO-PDMS coating can be attributed primarily to the hierarchical structure of the ZnO nanostructures and the PDMS polymer matrix. The vertically oriented ZnO nanoflakes increase mechanical interlocking and resist localized plastic deformation, resulting in improved surface hardness [28,29]. Meanwhile, the presence of PDMS,

a flexible polymer, moderates stress distribution and prevents abrupt brittleness, maintaining an adequate balance between hardness and ductility ^[30]. Consequently, the coating system exhibits increased durability without critically sacrificing the flexibility necessary for practical engineering applications. These observations suggest the nano-ZnO coating provides a significant improvement in mechanical properties, making it beneficial for applications requiring enhanced hardness and moderate ductility ^[31].

3.3. Wettability and hydrophobicity

The wettability and hydrophobic properties of AA6070, AA6070-ZnO, and AA6070-ZnO-PDMS surfaces were thoroughly evaluated through static contact angle (CA) and sliding angle (SA) measurements. Contact angle measurements reveal remarkable increases in surface hydrophobicity upon nano-ZnO and PDMS coating. The bare AA6070 alloy exhibited hydrophilic properties with an average water contact angle of approximately 78°. Upon hydrothermal ZnO coating, the surface showed a significant increase in hydrophilicity due to enhanced roughness, resulting in near-zero contact angles ^[32]. However, subsequent PDMS modification dramatically reversed this trend, creating a pronounced superhydrophobic surface with an average contact angle reaching approximately 162°, accompanied by an exceptionally low sliding angle of around 2.5°, indicating strong superhydrophobic behavior ^[33].

This observed transition from hydrophilicity to superhydrophobicity can be explained by the significant reduction in surface free energy upon PDMS treatment. PDMS, possessing numerous non-polar methyl groups, substantially reduces the surface energy, enabling the surface to resist water penetration effectively ^[34]. The Cassie-Baxter model explains this behavior, wherein air pockets trapped within the hierarchical ZnO structures reduce the solid-liquid contact area, further enhancing the hydrophobic effect. The extremely low surface free energy of approximately 1.45 mJ/m², as calculated using Owens' method, corroborates the excellent hydrophobicity.

3.4. Corrosion performance

The corrosion resistance of AA6070 surfaces before and after coating with nano-ZnO and PDMS was assessed using electrochemical and accelerated salt spray tests. Potentiodynamic polarization results (Figure 5a) indicated a significant shift of corrosion potential (E_{corr}) from -1.42 V for bare AA6070 to -0.73 V for AA6070-ZnO-PDMS, while the corrosion current density (i_{corr}) dramatically decreased from 8.76×10^{-6} A/cm² to 1.23×10^{-7} A/cm² (Table 2). This notable reduction in corrosion rate underscores the protective capability provided by the ZnO-PDMS composite coating.

Electrochemical impedance spectroscopy (EIS) analyses (Figure 5b and 5c) revealed higher impedance values for AA6070-ZnO-PDMS coatings (approximately 4500 $\Omega \cdot \text{cm}^2$) compared to bare alloy (around 230 $\Omega \cdot \text{cm}^2$). This result indicates the formation of a stable and effective barrier that limits electrolyte penetration and corrosion initiation.

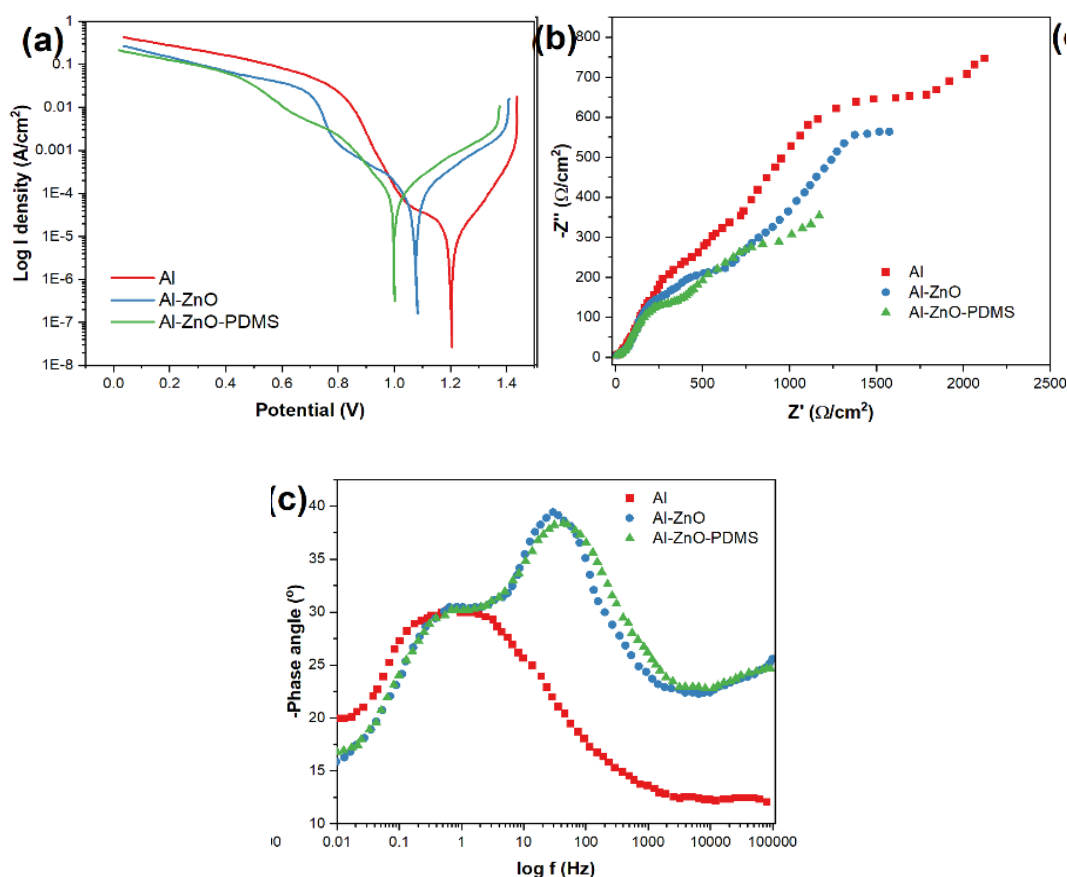


Fig. 5. (a) Polarization curves of coated vs. bare AA6070, (b) Nyquist plots, and (c) Bode impedance plots after corrosion tests.

Salt spray testing further validated these findings, demonstrating that after 400 hours, uncoated samples exhibited severe corrosion characterized by extensive pitting and oxide formation [35]. In contrast, AA6070-ZnO-PDMS surfaces displayed minimal corrosion damage, with only minor localized corrosion sites. XRD analysis (Figure 6) confirmed the formation of stable corrosion products such as simonkolleite ($\text{Zn}_5(\text{OH})_8\text{Cl}_2 \cdot \text{H}_2\text{O}$) and hydrozincite ($\text{Zn}_5(\text{CO}_3)_2(\text{OH})_6$), both providing enhanced corrosion protection by filling micro-pores and minimizing chloride ion ingress.

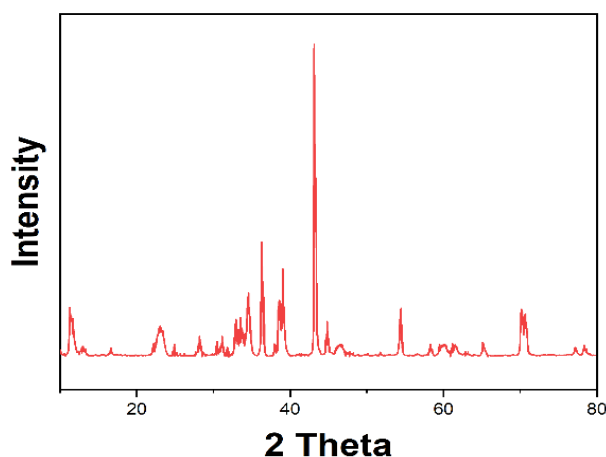


Fig. 6. XRD patterns identifying corrosion products formed after salt spray testing.

Table 2. Electrochemical parameters of AA6070 aluminum alloy samples before and after nano-ZnO and PDMS coating.

Sample	Corrosion Potential (E_{corr} , V)	Corrosion Current Density (i_{corr} , A/cm ²)	Polarization Resistance (R_p , $\Omega \cdot \text{cm}^2$)	Corrosion Rate (mm/year)
AA6070 (Bare)	-1.42 ± 0.04	$(8.76 \pm 0.42) \times 10^{-6}$	230 ± 15	0.102 ± 0.009
AA6070-ZnO	-0.89 ± 0.03	$(4.65 \pm 0.19) \times 10^{-7}$	1580 ± 65	0.057 ± 0.004
AA6070-ZnO-PDMS	-0.73 ± 0.03	$(2.81 \pm 0.12) \times 10^{-7}$	4500 ± 130	0.034 ± 0.003

4. Conclusion

In this study, nano-ZnO coatings were successfully applied to AA6070 aluminum alloys, significantly enhancing their surface properties, mechanical performance, and corrosion resistance. The hierarchical nano-ZnO structures, synthesized via a hydrothermal approach and modified with PDMS, substantially increased the surface hardness from 96 HV to 186 HV, representing an approximate 100% improvement. Despite this substantial enhancement, ductility exhibited a modest reduction, with elongation decreasing from 15.2% in uncoated alloys to 12.8% post-coating, indicating a favorable balance between hardness and ductility.

Corrosion resistance notably improved, demonstrated by a shift in corrosion potential from -1.42 V to -0.73 V and a substantial decrease in corrosion current density from 8.76×10^{-7} A/cm² to 2.81×10^{-7} A/cm². Additionally, the coatings exhibited superhydrophobic characteristics, with contact angles dramatically increasing from 78° to approximately 158°, thus significantly reducing surface wettability and enhancing anti-icing and self-cleaning functionalities.

These multifunctional properties, achieved through a hierarchical ZnO structure modified by PDMS, position nano-ZnO coatings as highly effective protective systems, promising enhanced

durability and operational performance of aluminum alloys in aggressive environments.

References

- [1] Zhang L C, Chen L Y, Wang L., *Advanced Engineering Materials*, 2020, 22(5): 1901258; <https://doi.org/10.1002/adem.201901258>
- [2] Quazi M M, Fazal M A, Haseeb A S M A, et al., *Critical Reviews in Solid State and Materials Sciences*, 2016, 41(2): 106-131; <https://doi.org/10.1080/10408436.2015.1076716>
- [3] Hu J, Zhang C, Wang X, et al., *Coatings*, 2024, 14(4): 476; <https://doi.org/10.3390/coatings14040476>
- [4] Voevodin N N, Balbyshev V N, Khobaib M, et al., *Progress in Organic Coatings*, 2003, 47(3-4): 416-423; [https://doi.org/10.1016/S0300-9440\(03\)00131-0](https://doi.org/10.1016/S0300-9440(03)00131-0)
- [5] Górka J, Lont A, Janicki D, et al., *Coatings*, 2024, 14(5): 646; <https://doi.org/10.3390/coatings14050646>
- [6] Bakhsheshi-Rad H R, Daroonparvar M, Yajid M A M, et al., *Journal of Materials Engineering and Performance*, 2021, 30(2): 1356-1370; <https://doi.org/10.1007/s11665-020-05333-4>
- [7] Kathavate V S, Pawar D N, Bagal N S, et al., *Journal of Alloys and Compounds*, 2020, 823: 153812; <https://doi.org/10.1016/j.jallcom.2020.153812>
- [8] Sarshar M A, Song D, Swartz C, et al., *Langmuir*, 2018, 34(46): 13821-13827; <https://doi.org/10.1021/acs.langmuir.8b02231>
- [9] Zuo Z, Song X, Liao R, et al., *International Journal of Heat and Mass Transfer*, 2019, 133: 119-128; <https://doi.org/10.1016/j.ijheatmasstransfer.2018.12.092>
- [10] Lin W, Cao M, Olonisakin K, et al., *Cellulose*, 2021, 28(16): 10425-10439; <https://doi.org/10.1007/s10570-021-04175-0>
- [11] Fürstner R, Barthlott W, Neinhuis C, et al., *Langmuir*, 2005, 21(3): 956-961; <https://doi.org/10.1021/la0401011>
- [12] Lin T Y, Zhang X Y, Huang X, et al., *Rare Metals*, 2018, 37(11): 976-982; <https://doi.org/10.1007/s12598-017-0948-z>
- [13] Zhu L, Li Y, Zeng W., *Applied Surface Science*, 2018, 427: 281-287; <https://doi.org/10.1016/j.apsusc.2017.08.229>
- [14] Huang K, Huang X, Wang L, et al., *Molecules*, 2024, 29(19): 4644; <https://doi.org/10.3390/molecules29194644>
- [15] Babaei K, Fattah-alhosseini A, Molaei M., *Surfaces and Interfaces*, 2020, 21: 100677; <https://doi.org/10.1016/j.surfin.2020.100677>
- [16] Bayuseno A P, Schmahl W W., *Journal of Crystal Growth*, 2018, 498: 336-345; <https://doi.org/10.1016/j.jcrysgro.2018.06.026>
- [17] Lao J Y, Wen J G, Ren Z F., *Nano Letters*, 2002, 2(11): 1287-1291; <https://doi.org/10.1021/nl025753t>
- [18] Kim J H, Mirzaei A, Kim H W, et al., *Applied Surface Science*, 2018, 451: 207-217; <https://doi.org/10.1016/j.apsusc.2018.04.187>
- [19] Beshkar F, Khojasteh H, Salavati-Niasari M., *Materials*, 2017, 10(7): 697;

<https://doi.org/10.3390/ma10070697>

- [20] Wang T, Lu Z, Wang X, et al., Applied Surface Science, 2021, 550: 149286;
<https://doi.org/10.1016/j.apsusc.2021.149286>
- [21] Tropmann A, Tanguy L, Koltay P, et al., Langmuir, 2012, 28(22): 8292-8295;
<https://doi.org/10.1021/la301283m>
- [22] Martin S, Bhushan B., Journal of Colloid and Interface Science, 2017, 488: 118-126;
<https://doi.org/10.1016/j.jcis.2016.10.094>
- [23] Chen C, Tian Z, Luo X, et al., ACS Applied Materials & Interfaces, 2022, 14(20): 23973-23982; <https://doi.org/10.1021/acsami.2c02992>
- [24] Kesler D, Ariyawansa B P, Rathnayake H., Polymers, 2023, 15(6): 1522;
<https://doi.org/10.3390/polym15061522>
- [25] Rai R S, Bajpai V., Polymer Composites, 2024, 45(3): 2012-2031;
<https://doi.org/10.1002/pc.27901>
- [26] Konstantinov V M, Kovalchuk A V., Science & Technique, 2020, 19(6): 480-491;
<https://doi.org/10.21122/2227-1031-2020-19-6-480-491>
- [27] Zhao P, Shi Z, Wang X, et al., Lubricants, 2023, 11(11): 482;
<https://doi.org/10.3390/lubricants11110482>
- [28] Son N T, Noh J S, Park S., Applied Surface Science, 2016, 379: 440-445;
<https://doi.org/10.1016/j.apsusc.2016.04.107>
- [29] Ahmad R, Majhi S M, Zhang X, et al., Advances in Colloid and Interface Science, 2019, 270: 1-27; <https://doi.org/10.1016/j.cis.2019.05.006>
- [30] Sarma S, Srivastava R., Polymer Composites, 2024, 45(10): 9461-9470;
<https://doi.org/10.1002/pc.28420>
- [31] Kabaoglu E, Karabork F, Balun Kayan D, et al., Journal of Composite Materials, 2023, 57(3): 451-463; <https://doi.org/10.1177/00219983221146846>
- [32] Jeong S W, Bolortuya S, Eadi S B, et al., Journal of Adhesion Science and Technology, 2020, 34(1): 102-113; <https://doi.org/10.1080/01694243.2019.1661609>
- [33] Chakraborty A, Gottumukkala N R, Gupta M C., Langmuir, 2023, 39(32): 11259-11267;
<https://doi.org/10.1021/acs.langmuir.3c00818>
- [34] Koşak Söz Ç, Trosien S, Biesalski M., ACS Applied Materials & Interfaces, 2018, 10(43): 37478-37488; <https://doi.org/10.1021/acsami.8b12116>
- [35] R. Kamalakannan B A., International Journal of Scientific & Technology Research, 2020, 9: 462-465.